Supporting Information

High-performance p-n junction transition metal dichalcogenide photovoltaic cells enabled by MoO_x doping and passivation

Koosha Nassiri Nazif,[1] Aravindh Kumar,[1] Jiho Hong,[2,3] Nayeun Lee,[2,3] Raisul Islam,[1] Connor J. McClellan,[1] Ouri Karni,[4] Jorik van de Groep,[2,5] Tony F. Heinz,[4,1] Eric Pop,[1,3] Mark L. Brongersma,[2,3,4] and Krishna C. Saraswat[1,3*]

[1]Department of Electrical Engineering, Stanford University, Stanford, CA 94305, USA
[2]Geballe Laboratory for Advanced Materials, Stanford University, Stanford, CA 94305, USA
[3]Department of Materials Science and Engineering, Stanford University, Stanford, CA 94305, USA
[4]Department of Applied Physics, Stanford University, Stanford, CA 94305, USA
[5]Institute of Physics, University of Amsterdam, 1098 XH Amsterdam, The Netherlands
*email: saraswat@stanford.edu

This file includes:

Section S1. Detailed WS_2 Transfer Procedure

Polydimethylsiloxane (PDMS, Dow Corning Sylgard™ 182) - is mixed in a glass petri dish and left in a vacuum desiccator for 48 hours to remove air bubbles and create a flat surface. PDMS is then cut into 0.5 x 0.5 cm squares with a razor blade. Each square is removed from the petri dish and placed on thin, transparent 2 x 2 cm plastic sheet. Polypropylene carbonate - PPC (Sigma-Aldrich) - was dissolved into anisole (Sigma-Aldrich) with a weight ratio of 15% PPC: 85% anisole and left on a 60°C hot plate for 24 hours in the ambient air. A drop of PCC is spin-coated on the

PDMS stamp (4000 rpm for 45 seconds). The PDMS/PPC stack is subsequently placed on a 200 °C hot plate in the ambient air for 2 minutes to further solidify PPC and improve PPC/PDMS adhesion. As shown in Fig. S1, WS_2 flakes are exfoliated from a WS_2 crystal (2D Semiconductors) using low-residue thermal release tape (Nitto Denko REVALPHA), and then picked up (exfoliated) by Gel-Film® (Gel-Pak, WF-20-X4) and transferred (exfoliated) onto the PDMS/PPC stamp. Because the WS_2 flake is being exfoliated with each transfer step, the outer surface of the flakes – not in contact with PPC - is clean and free of tape or Gel-Film® residue. The PDMS/PPC stamp is aligned and laminated onto the bottom contact under an optical microscope. The stage is heated to 90°C, above the transition temperature of PPC. After thermal equilibrium, the stamp is removed quickly, leaving the WS_2 flake behind on the substrate. The PPC residue is dissolved and removed by placing the sample in acetone for 4 minutes.

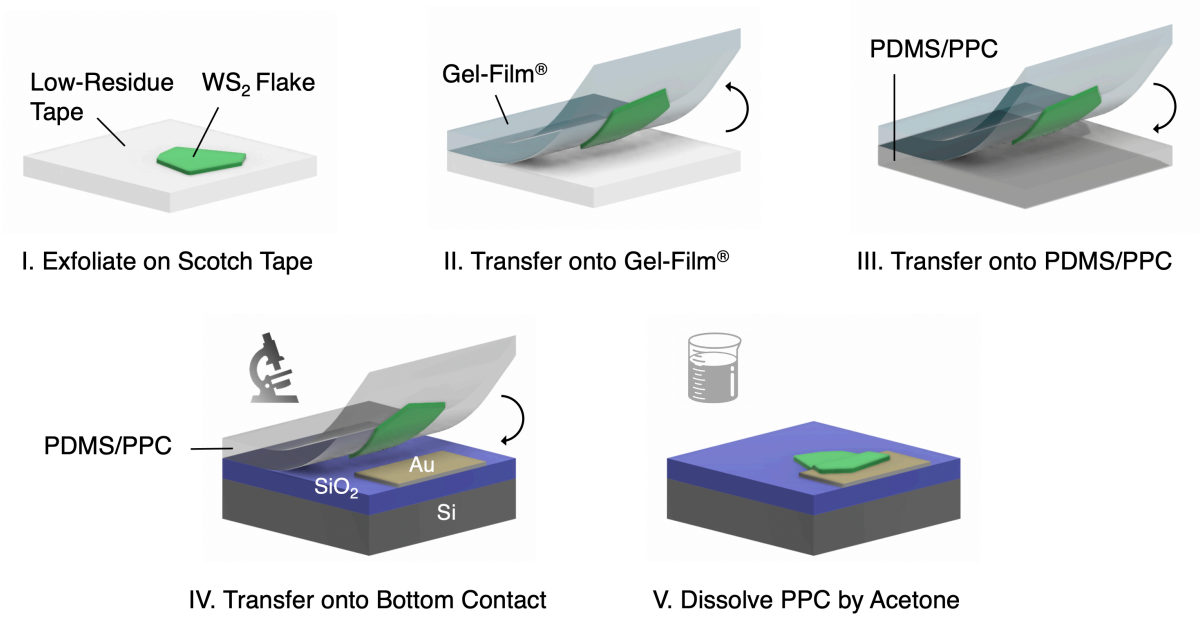

Figure S1 I WS_2 Transfer Process. (**I**) WS_2 flake is exfoliated from a WS_2 crystal onto a low-residue thermal release tape. The flake is (**II**) picked up by a Gel-Film® and then (**III**) transferred onto a polydimethylsiloxane (PDMS)/polypropylene carbonate (PPC) stamp. (**IV**) The PDMS/PPC stamp is aligned and laminated onto the bottom contact and then removed quickly above the glass transition temperature of PPC, leaving the WS_2 behind. (**V**) The PPC residue is dissolved and removed by placing the sample in acetone for 4 minutes.

Section S2. Doping density estimate

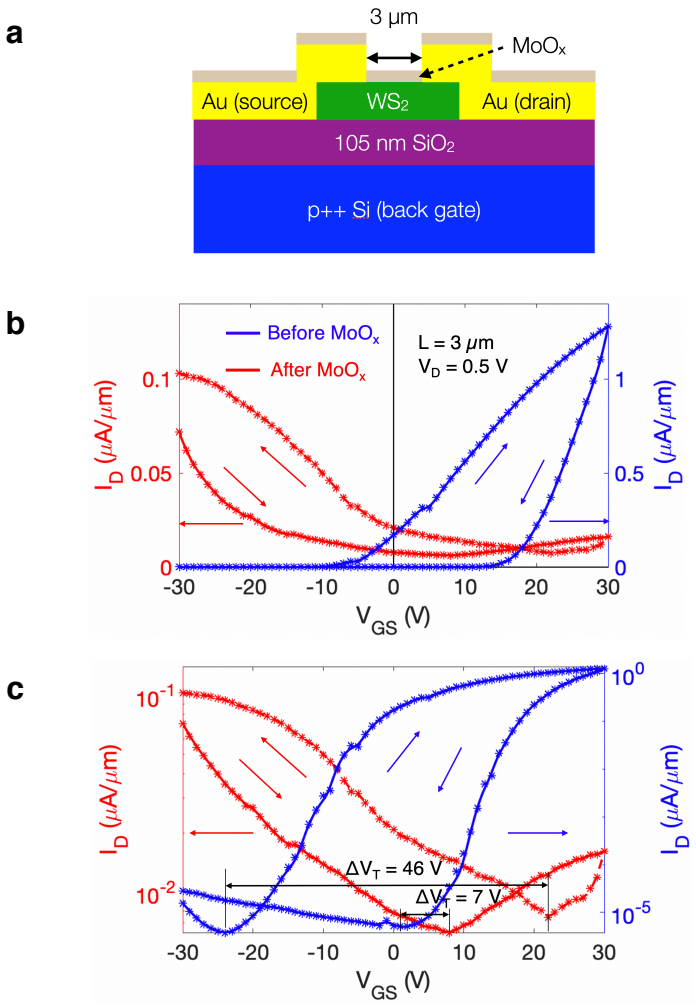

Figure S2 l Doping density estimate. (**a**) Schematic cross-section of a WS_2 field-effect transistor (FET) along with its (**b-c**) forward and reverse I_D vs. V_{GS} (drain current vs. gate voltage) sweeps measured in air, before (blue) and after (red) MoO_x capping, in (b) linear and (c) logarithmic scales. Sweep directions are shown by the arrows. Device has hysteresis, due to trap states at SiO_2-WS_2 and WS_2-air interface. By passivating the trap states at the top surface of WS_2, MoO_x capping reduces hysteresis. The change in channel doping after MoO_x capping (p) can be estimated as $p \approx C_{ox}\Delta V_T/q$, where $C_{ox} \approx 33$ nF/cm^2 is the gate oxide capacitance, ΔV_T is the difference between threshold voltages before and after MoO_x, and q is the elementary charge. ΔV_T is estimated here by the difference between voltages of the transition points (I_D-V_{GS} minima). A large increase in hole concentration is observed after MoO_x, with a lower bound of 1.4×10^{12} cm^{-2} (corresponding to $\Delta V_T = 7$ V) and an upper bound of 9.5×10^{12} cm^{-2} (corresponding to $\Delta V_T = 46$ V).

Section S3. EQE measurement at infrared wavelengths

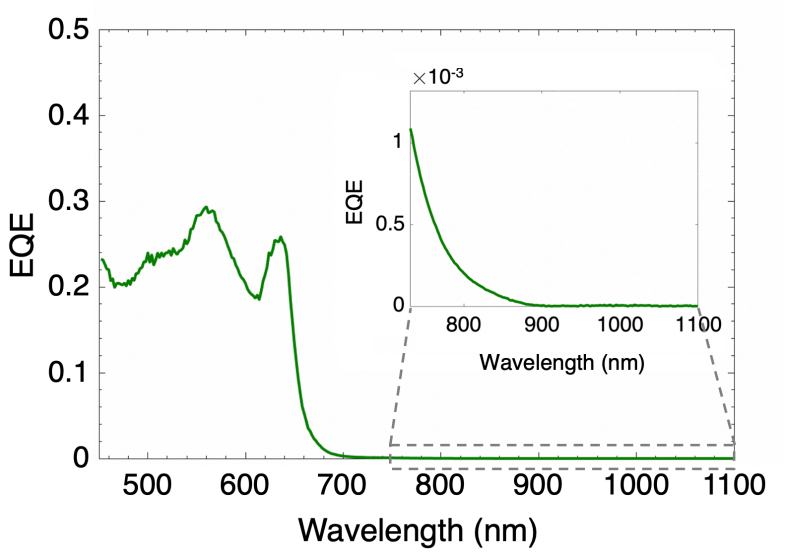

Figure S3 | EQE measurement at infrared wavelengths. EQE measured at a 2-μm-diameter spot within the device active area (Point S in Fig. 3a). Inset shows a zoomed-in view of the infrared 750-1100 nm wavelength regime, which is used to extract the bandgap of multilayer WS_2 (Fig. 3d).

Section S4. Reproducibility

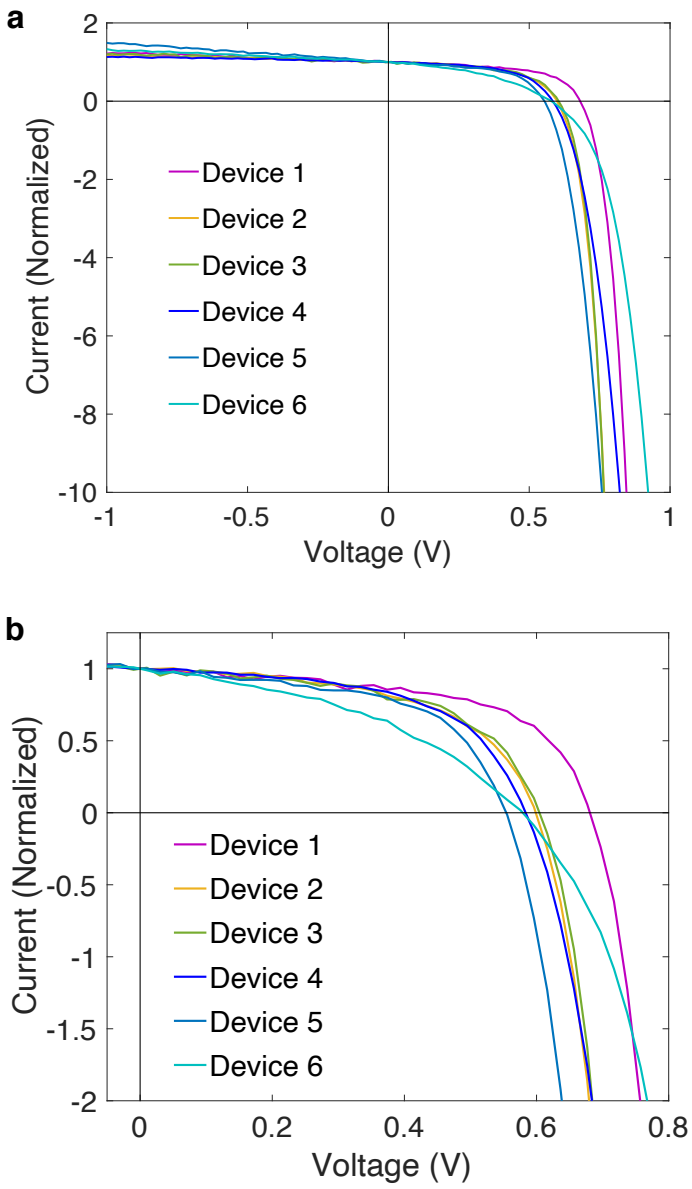

Figure S4 I Reproducibility. (**a**) I-V characteristics of 6 different devices under AM 1.5G illumination. V_{OC} is between 554 mV and 681 mV across all devices. (**b**) Zoomed-in view of the photovoltaic region. Current levels vary across devices due to their different thicknesses and active areas as well as process variability. For easier comparison, current is therefore normalized by the short-circuit current.

Section S5. Forward and backward scans

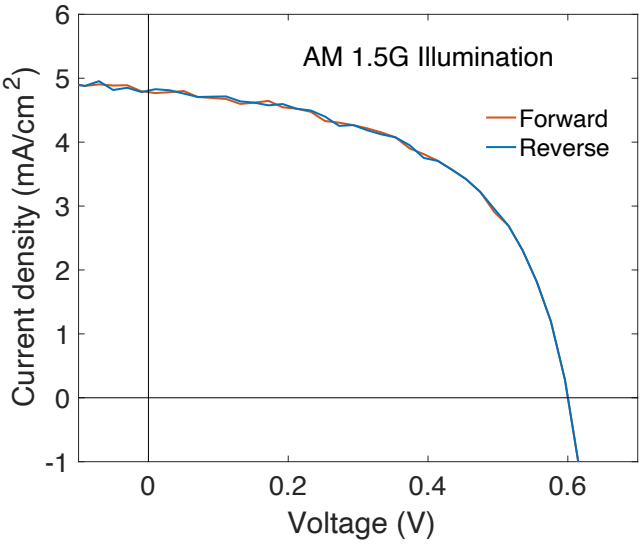

Figure S5 I Forward and backward scans. I-V characteristics under one-sun illumination show no hysteresis in forward/reverse voltage sweeps.

Section S6. Thickness-dependent absorption in WS_2

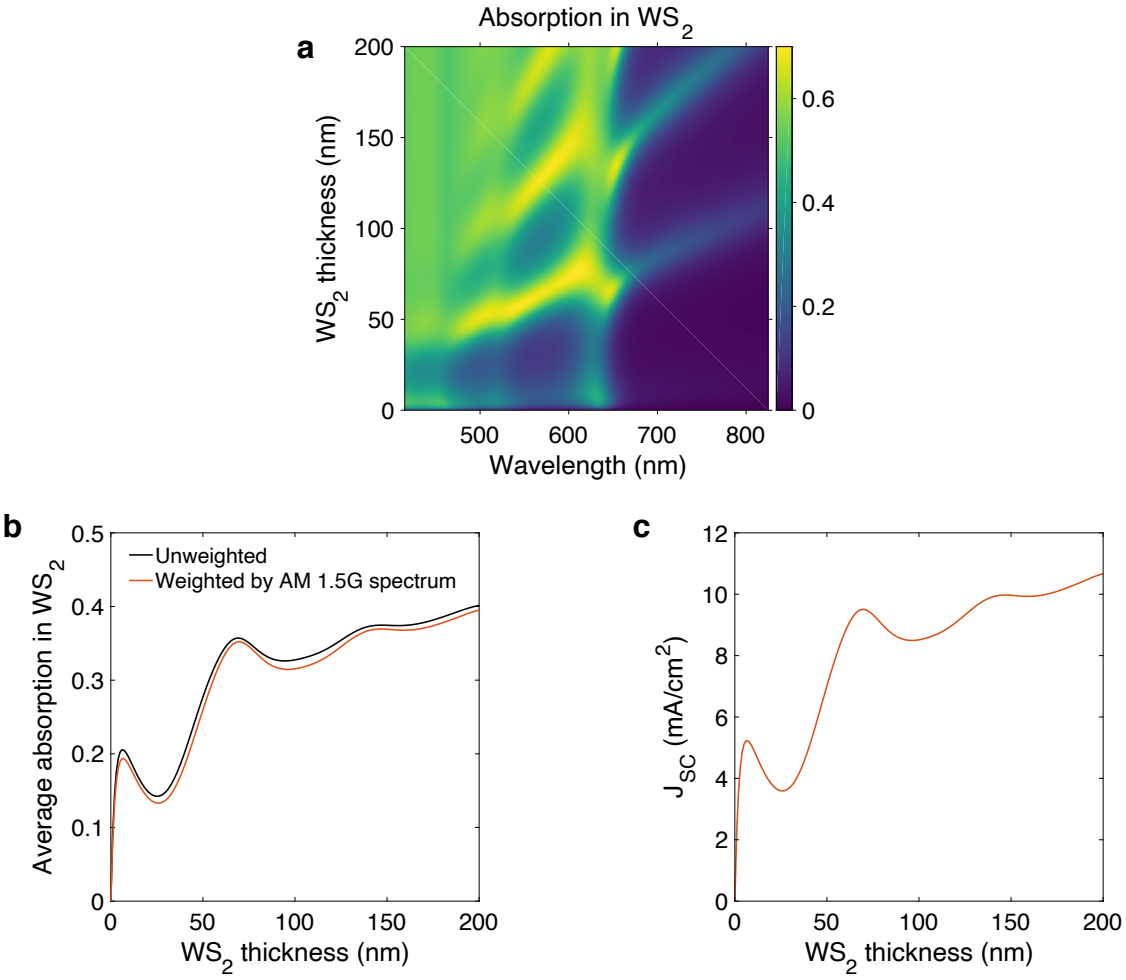

Figure S6 | Thickness-dependent absorption in WS_2. (**a**) Absorption spectrum of WS_2 in a Si-SiO_2-WS_2-MoO_x stack as a function of WS_2 thickness, simulated using the transfer matrix method. (**b**) Unweighted and weighted (by AM 1.5G spectrum) average of absorption in WS_2 as a function of WS_2 thickness. 70-nm-thick WS_2 has the highest average absorption (~35%) in the sub-100-nm thickness regime. (**c**) Maximum short-circuit current density (J_{SC}) attainable from WS_2 in the Si-SiO_2-WS_2-MoO_x stack as a function of WS_2 thickness, calculated by integrating Absorption(λ) × (spectral photon flux of AM1.5G spectrum at 1-sun solar intensity) over the wavelength range of λ = 415-825 nm, assuming unity IQE. This maximum J_{SC} value is slightly underestimated as absorption at wavelengths below 415 nm and above 825 nm are not included due to lack of material data.

Section S7. 2D finite-element device physics simulation

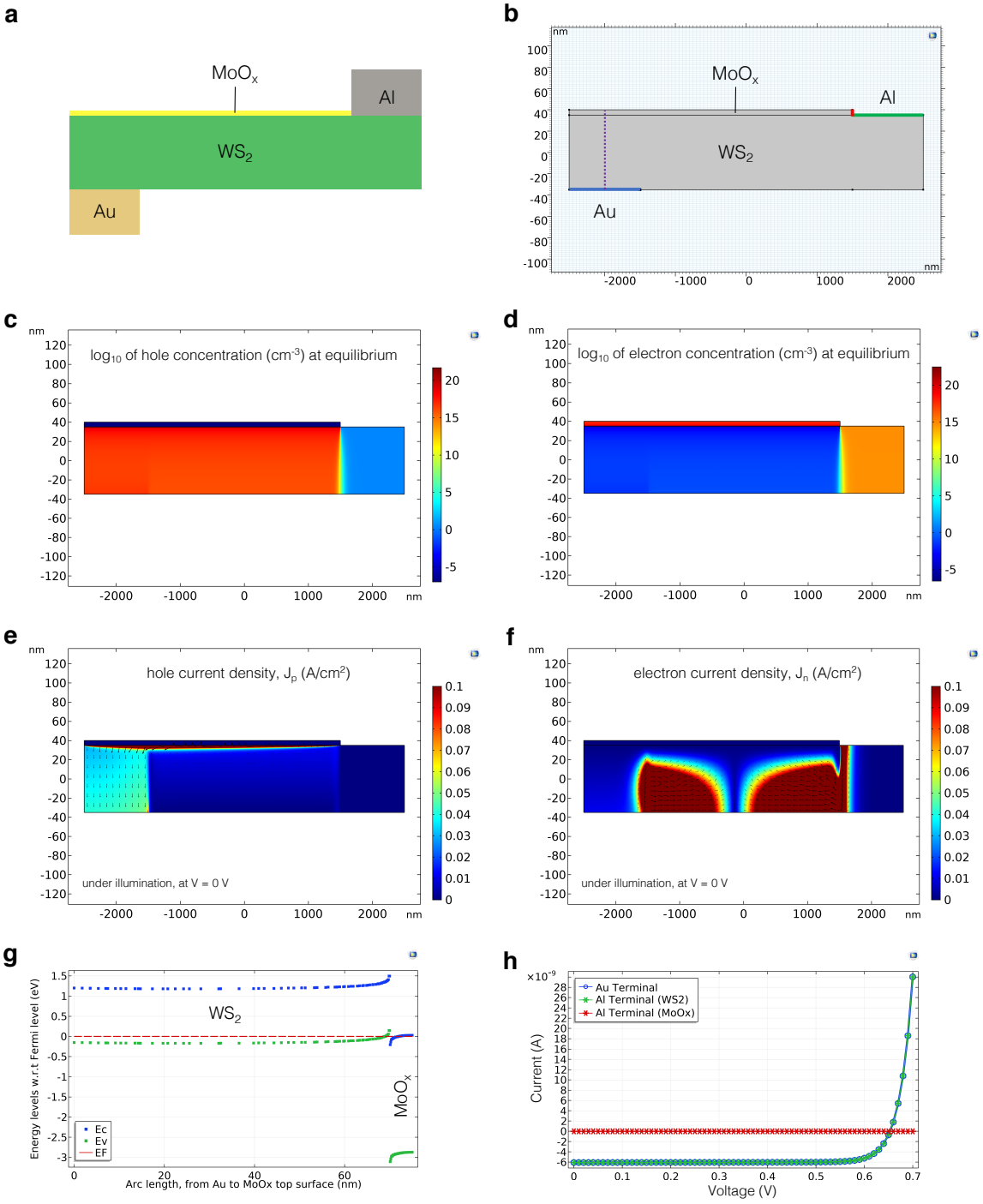

Figure S7 I 2D finite-element device physics simulation. (**a**) Schematics of the simplified device structure used in the finite-element device physics simulation study. (**b**) Simplified device structure simulated in COMSOL Multiphysics 5.4 semiconductor module. (**c-d**) Log_{10} of (c) hole and (d) electron concentration at equilibrium, showing strong charge transfer doping of WS_2 by MoO_x. (**e-f**) (e) Hole and (f) electron current density under illumination at zero applied bias.

(**g**) Equilibrium band diagram of the device along the purple dotted line shown in panel (b), demonstrating the vertical doping gradient in WS_2. (**h**) I-V curve of the simulated device under illumination, showing good agreement with the experiments. To simulate illumination, a constant photogeneration rate of 10^{22} cm^{-3}·s was assumed in the WS_2 regions not shaded by the Al contact. To achieve $V_{OC} > 650$ mV in this simplified model, Al work functions of 4.25 eV and lower were needed. Au work function was assumed to be 5.2 eV. In conjunction with panel (e) and (f), the plot also shows that all current flows through WS_2 (no conduction through MoO_x) even if the highly electron-doped MoO_x (panel (d)) is touching the Al contact on the side. Au terminal (blue) and Al terminals contacting WS_2 (green) and MoO_x (red) are highlighted in panel (b) using the same color code.